AIAA Guidance, Navigation and Control Conference and Exhibit
18 - 21 August 2008, Honolulu, Hawaii

AIAA 2008-7221

Applications of a Macroscopic Model for En Route Sector Capacity

Jerry D. Welch[1], John W. Andrews[2], Brian D. Martin[3], and Eric M. Shank[4]
M.I.T. Lincoln Laboratory, Lexington, MA 02420-9108

Airspace capacity estimates are important both for airspace design and for operational air traffic management. Considerable effort has gone into understanding the complexity factors that reduce sector capacity by increasing controller workload. Yet no analytical means is available for accurately estimating the maximum capacity of an en route sector. The Monitor Alert Parameter (MAP) values that determine the operational traffic limit of en route sectors in the United States account only for workload from inter-sector coordination tasks. We propose a more complete sector capacity model that also accounts for workload from conflict avoidance and recurring tasks. We use mean closing speeds and airspace separation standards to estimate aircraft conflict rates. We estimate the mean controller service times for all three task types by fitting the model against observed peak traffic counts for hundreds of en route airspace volumes in the Northeastern United States. This macroscopic approach provides numerical capacity predictions that closely bound peak observed traffic densities for those airspace volumes. This paper reviews recent efforts to improve the accuracy of the bound by replacing certain global parameters with measured data from individual sectors. It also compares the model capacity with MAP values for sectors in the New York Center. It concludes by illustrating the use of the model to predict the capacity benefits of proposed technological and operational improvements to the air traffic management system.

Nomenclature

F	=	daily fraction of sector aircraft with altitude change ≥ 2000 ft
G	=	workload intensity
G_b	=	background workload intensity
M_h	=	horizontal miss distance
M_v	=	vertical miss distance
M_{vmax}	=	vertical miss distance when all aircraft have vertical rates
N	=	sector aircraft count
N_b	=	sector aircraft count predicted by model
N_p	=	peak measured sector aircraft count
P	=	recurring task period
Q	=	sector volume
S	=	mean speed of sector traffic
T	=	mean transit time for sector traffic measured when $N = N_p$
τ_c	=	mean service time for conflict tasks
τ_r	=	mean service time for recurring tasks
τ_t	=	mean service time for transit tasks
V_{21}	=	mean pair-wise closing speed of sector traffic

[1] Senior Staff, Surveillance Systems Group, S2-527G, non-member.
[2] Senior Staff, Surveillance Systems Group, S2-527H, non-member.
[3] Assistant Staff, Weather Sensing Group, S1-670, Member.
[4] Staff, Surveillance Systems Group, S2-509, non-member.

I. Introduction

Knowledge of airspace capacity is needed to mitigate delay from storms, demand peaks, and operations growth. Capacity estimates are also key tools for airspace design and for guiding the development of controller decision support tools.

There is broad agreement that controller workload is the main determinant of en route sector capacity.[1-9] Many studies have focused on understanding the dynamic complexity factors that reduce sector capacity.[1-14] These have largely been efforts to identify and rank all sources of complexity that can increase controller workload.

There has been little focus on accurately determining inherent, un-reduced sector capacity. As a result, Federal Aviation Administration (FAA) air traffic managers do not have an accurate means for estimating the safe traffic limit of en route sectors in an operational environment. The current FAA Monitor Alert Parameter (MAP) rule for determining maximum operational sector loading considers only the inter-sector coordination component of controller workload.[15] The rule sometimes allows what would be dangerously high traffic densities in small sectors because it does not account for separation assurance workload. It also arbitrarily limits peak sector counts to eighteen aircraft. This tends to underestimate the actual safe capacity of many large sectors.

We previously reported[16] a method of estimating maximum capacity by extending and inverting an established queuing model[17] that accounts not only for workload from inter-sector coordination but also from efforts to assure safe aircraft separation. The model uses mean closing speeds and effective separation standards to estimate aircraft conflict rates. The capacity of a given airspace sector is reached when the sum of the products of the event rates and service times approaches unity, indicating that the controller team is fully occupied.

The model is "macroscopic" in the sense that it assumes a common global controller service time for all inter-sector coordination tasks and another global service time for all aircraft separation tasks. The analytical nature of the model facilitates the process of inferring controller service times for these tasks by fitting against peak traffic counts from large numbers of actual en route sectors. The result is a formula for estimating peak allowable sector aircraft count based on aircraft speeds, sector geometry, and airspace separation standards.

We first used the model in its original workload context to study the variability of controller workload in a free-flight environment.[18] In Ref. 16 we inverted the workload equation to determine capacity and extended the task types to include background and recurring tasks, thereby providing a complete set of workload generating events.

We compared the resulting model capacity values with peak, clear-weather operational traffic counts from 425 sectors in the Corridor Integrated Weather System (CIWS) airspace domain in the Northeast United States.[19] We obtained the coordinates of the CIWS sectors from the FAA's Enhanced Traffic Management System (ETMS) graphical plotting database. Many of these "ETMS/CIWS" sectors are smaller in airspace volume than actual operational sectors because the two-dimensional ETMS plots include only one sub-module from each sector.

The comparison of the model with peak traffic was unaffected by this size discrepancy because we based the model capacities and the peak sector traffic counts on consistent airspace coordinates. We found that the model capacity values closely bounded the peak operational traffic counts. However, the ETMS/CIWS volume discrepancy prevented us from comparing the model capacity with the operational FAA MAP value for each sector. We have thus begun a comparison of operational MAP values with model capacity values based on accurate sector coordinates. We include initial comparison results in this paper for sectors in the New York Air Route Traffic Control Center (ZNY).

We also describe recent efforts to improve the model by using traffic measurements from individual sectors to replace what were originally global assumptions. We originally estimated transit time based on sector length and an assumed constant aircraft transit speed. Observing actual flight times in each sector in peak traffic periods allows us to determine transit time directly. We originally assumed that all aircraft were in level flight. Observation of the fraction of tracks with significant vertical motion in each sector allows us to account for increased workload caused by climbing and descending aircraft. Both of these improvements increase the number of sectors whose observed traffic peaks agree with the capacity bound.

We conclude with an illustration of the use of the model to estimate the expected capacity benefits of hypothetical technological, automation, and operational improvements to today's air traffic management system.

II. The Capacity Model

A. Model Structure

The model is based on a simple queuing principle: the product of the occurrence rate of a task and the time required to complete that task is the task's "workload intensity" or the fraction of the available time in which the controller team is busy executing that task.

The model aggregates controller tasks into four types differentiated according to occurrence characteristics. This allows any controller activity to be uniquely assigned to one task type. The four types are background, transition, recurring, and conflict.

Background tasks cause a constant workload intensity G_b without respect to the aircraft count in the sector.

The rates of transition tasks, which occur when aircraft enter or exit the sector, and recurring tasks, which occur repeatedly for each aircraft in the sector, are both proportional to the sector traffic count. Transition tasks occur at a rate

$$\lambda_t = N/T, \tag{1}$$

where N is the number of aircraft in the sector, and T is the average transit time through the sector. Recurring tasks occur at a rate

$$\lambda_r = N/P, \tag{2}$$

where P is the mean task recurrence period per aircraft.

Conflict workload occurs when potential aircraft separation violations arise. For uniformly distributed traffic, the conflict rate as perceived by the sector controller team increases as the square of the sector traffic count. The mean conflict rate is

$$\lambda_c = (2\ N^2/Q)\ M_h M_v V_{12}, \tag{3}$$

where Q is the sector volume, M_h and M_v are the horizontal and vertical miss distances that define a separation violation, and V_{12} is the mean of the pair-wise closing speeds of the aircraft in the sector.

The total workload intensity G is the fraction of the controller's available time devoted to all four of these task types:

$$G = G_b + \tau_t\lambda_t + \tau_r\lambda_r + \tau_c\lambda_c, \tag{4}$$

where τ_t, τ_r, and τ_c are the mean times required to service transit, recurring, and conflict tasks, respectively. There is a critical total workload intensity, typically 0.8, beyond which a controller team cannot safely accept additional traffic. This queuing limit defines the traffic capacity of the sector. For each sector, we equate G to 0.8 and solve the resulting quadratic equation for N to determine its traffic capacity.

B. Model Parameters

Initially, we used global values for all of the sector workload parameters except T and Q. We estimated the global constants G_b, P, S, M_h, M_v, and V_{12} based on data from dense en route airspace in the Northeast United States. We estimated the transit time T of each sector based on its maximum horizontal length and an assumed constant global aircraft speed S. We computed the volume Q of each sector from its ETMS sector coordinates.

C. Regression Fitting to the Bound

We determined the values of the transit, conflict, and recurring work times by regression fitting the model to peak, clear-weather operational traffic counts for the ETMS/CIWS sectors.

Because the model provides a capacity *bound*, we used an asymmetric scoring scheme for regression fitting. Figure 1 graphs the scheme. It is a piece-wise linear scoring rule with parameters chosen to reward sectors with counts within plus or minus two aircraft of the bound and to strongly penalize those with counts that exceed the bound by more than 2 aircraft. We assume that sectors with peak counts N_p more than 2 aircraft below the integer-rounded model bound N_b are limited by low demand or other capacity constraints and thus do not count against the score. Each sector with $N_p = N_b$ increases the score by 3. Sectors with $N_p = N_b \pm 1$ increase the score by 2. Sectors with $N_p = N_b \pm 2$ increase the score by 1. Sectors with $N_p = N_b$+j score 1-10(j-2) for all integers j>2. We examined other combinations of rule parameters to adjust the location and tightness of the bound. Most combinations produced similar τ values for the ETMS/CIWS sectors.

To simplify the search, we stepped τ_t, τ_c, and τ_r in 1-second increments. This quantization, plus the variance of the measured data, caused the rule to occasionally return multiple identical local scoring maxima. The rule usually produced a distinct maximum score when fitting for τ_t. However, as we refined the model to account for measured

sector transit times and fractions of aircraft with vertical rates, the increased variance of the model data caused the rule to return nearly identical scores over a wider range of τ_c values. To minimize the number of sectors with counts that exceed the bound we chose the smallest τ_c value that maximized the score.

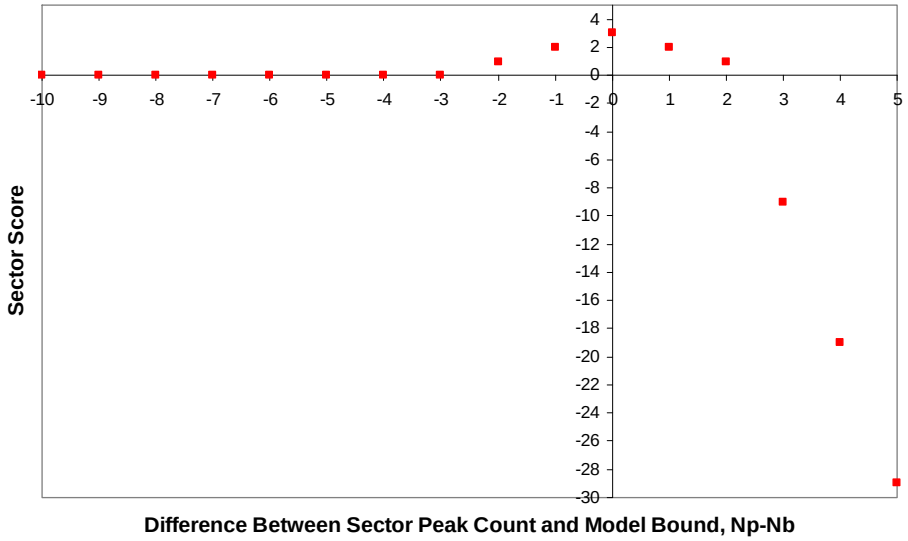

Figure 1. Rule for scoring a fit to the bound.

D. Results for Model Which Uses Sector Length to Estimate Transit Time

Figure 2 plots the model predictions of sector traffic capacity versus sector volume for each ETMS/CIWS sector when we use maximum sector horizontal length to estimate sector transit time *T*. The scatter in the model capacities for sectors with nearly identical airspace volumes is caused entirely by variations in maximum sector length. The figure also includes the observed peak traffic for each sector at its time of peak demand. Figure 3 directly plots the model capacities and the actual peak sector traffic counts versus each other. Low traffic demand and other factors caused many sectors to peak at densities below the modeled capacity. However, the "frontier" trend for their *maximum* count is consistent with the model.

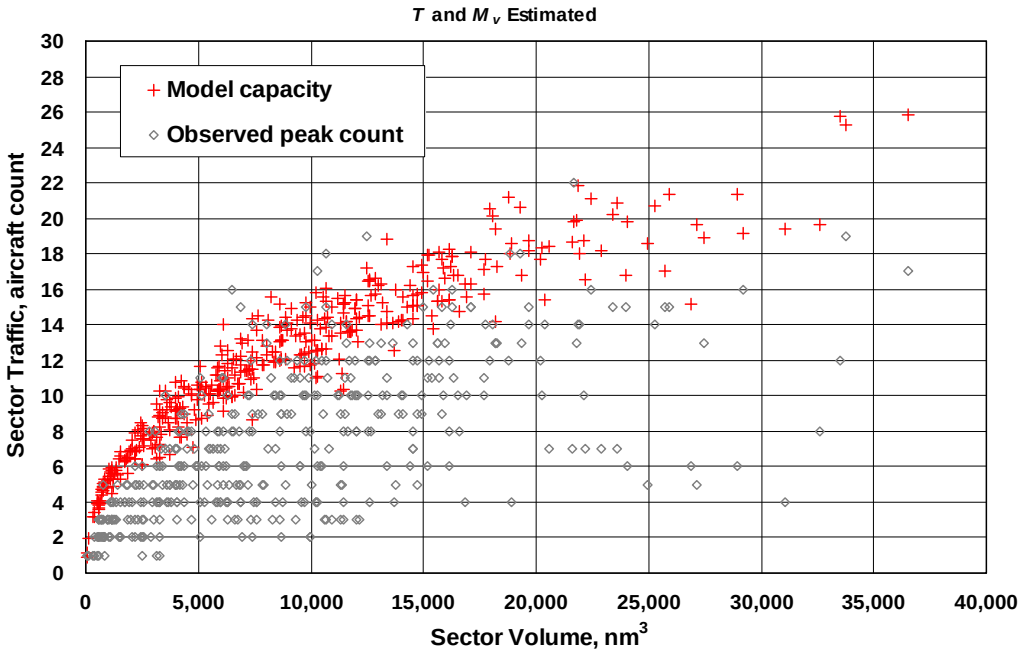

Figure 2. Peak counts and model capacities vs. sector volume when transit time is estimated from sector length.

In Ref. 16 we reported that the recurring work time τ_r was 2 seconds. This result was based on a preliminary regression analysis that identified a local maximum and failed to correctly fit τ_r. When we refined the procedure for fitting the bound to the sectors, the best fit consistently occurred for $\tau_r = 0$ s, indicating that recurring workload is insignificant relative to transit and conflict workload in those sectors. Ref. 16 also used a mean conflict closing speed of 440 kt (based on an analysis of conflict rates in future unstructured airspace) and a horizontal miss distance of 5 nautical miles. In busy regions of today's structured airspace, closing speeds of 200 kt and horizontal miss distances of 7 nm are more appropriate. With these changes, the transit and conflict work times that best fit the observed ETMS/CWIS peak sector counts are respectively 25 s and 104 s when the model capacity is determined by sector length.

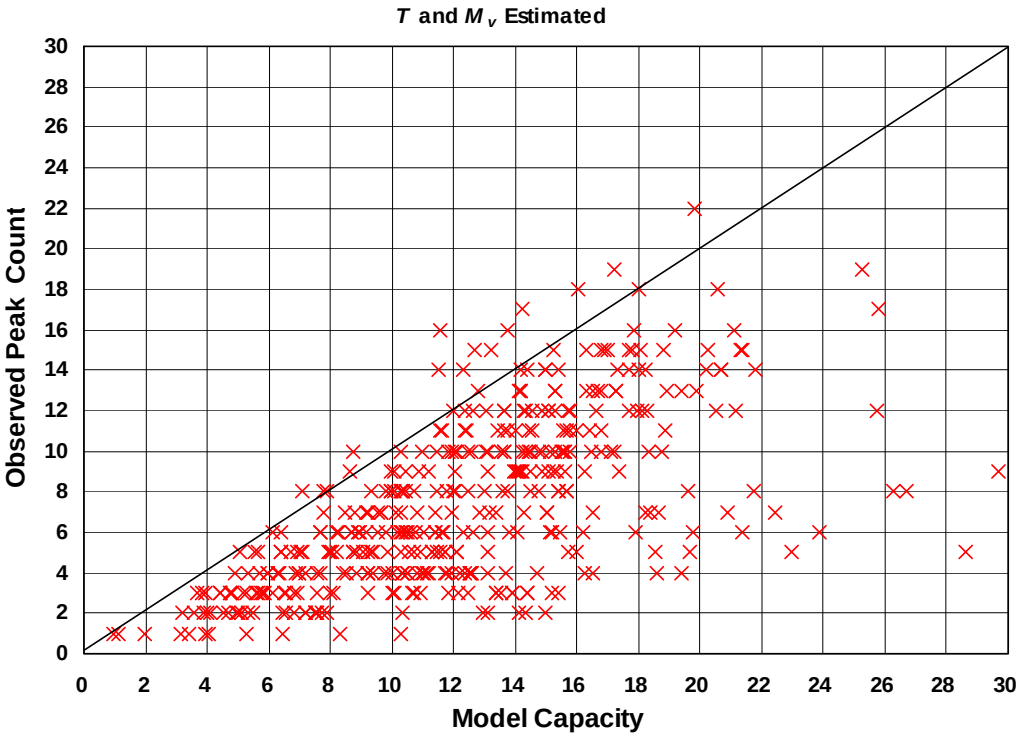

Figure 3. Peak Count vs. model capacity when transit time is estimated from sector length.

Using these values, sixteen sectors measured peak values in perfect agreement with the model. The number of close-fit sectors (defined as those for which the model fits the measured peak within ±2 aircraft) was 115. Two sectors had high peak counts (more than 2 aircraft above the bound) and 308 sectors (72% of the total) had low peak counts (more than 2 aircraft below the bound). The overall quality-of-fit score was 155.

E. Adding Measured Transit Time Data

We subsequently examined the tracks in each ETMS/CIWS sector and measured the the mean transit time T of the aircraft in each sector at the time of peak traffic. Local variations in transit time can either increase or decrease sector capacity. The use of measured T values increases the scatter in the model capacities for sectors with identical airspace volumes. Fast traffic or traffic using short-cut routes across the sector decrease the mean transit time T. On the other hand, speed reductions, holding patterns, S-turns, and vertical motion can temporarily increase T and hence sector capacity. Accounting for these variations allows the model to explain sectors with either high or low counts.

After adding measured sector transit times to the model, we re-ran the regression to determine the new global work times. The best fit for transit work time τ_t and recurring work time τ_r remained essentially unchanged. The increased variance of the model data caused the best fit for conflict work time τ_c to drop from 104 s per conflict to 82 s per conflict.

The use of measured transit time improved the model fit. The number of sectors with peak counts in perfect agreement with the model increased from 16 to 22, and the number of close-fit sectors increased from 115 to 169. Two additional sectors had high counts, but the number of sectors with low counts dropped from 308 to 252. The overall regression score increased from 155 to 229.

III. Sectors with Low Peak Traffic Counts

Some sectors may not have experienced enough peak demand to reach the bound because of traffic flow management or airline schedule restrictions. Others may have been affected by local workload factors that caused the model parameters for the sector to deviate from the global model values. Speed, heading, or altitude changes in a sector can increase workload by increasing trajectory uncertainty. Future positional uncertainty can increase the perceived conflict rate. Intersecting and converging routes within a sector can increase the conflict rate by increasing the mean closing speed V_{21}.

Several studies have determined that the major cause of increased sector workload is a high incidence of aircraft with vertical rates.[1,5,6,8,10] There is ample justification for this conclusion. The least predictable aircraft maneuver is an altitude change. The maximum climb rate is determined by factors that are often unknown to the controller. The climb or descent profile may take many forms. The start time or level-off time can vary. Aircraft may overshoot target altitudes. Thus, when aircraft move vertically, controllers must allow for increased altitude uncertainty in conflict planning, sometimes buffering all of the altitudes between current and planned cruise.

Majumdar et al studied candidate complexity factors using Eurocontrol simulation data. [6,10] They used real-time simulations of a single European sector with traffic operating under a wide range of conditions and found a strong correlation between reduced sector capacity and the simple fraction of ascending and descending aircraft in the sector.

We investigated this correlation for all 425 ETMS/CIWS sectors by comparing their observed peak traffic counts with predictions of the capacity model modified to account for the measured fraction of ascending and descending aircraft in the sector.

A. Measuring Vertical Motion

To estimate the operational effect of vertical rates on our capacity model, we examined tracks in the ETMS/CIWS sectors to determine a daily fraction of ascending and descending aircraft for each sector. We counted aircraft with altitude changes within a sector by identifying the entry and exit reports for each aircraft ID. We counted each track through a sector as one aircraft. If the entry and exit reports differed by more than 2000 feet, we counted the aircraft as having changed altitude. If an aircraft (using aircraft ID as the track identifier) remained in a sector for some period of time, then left for at least 5 minutes and subsequently reappeared, we considered the reappearance as a separate trip through the sector. We counted all aircraft that appeared in the data within the geographic boundary of each sector. According to this measure, 94% of the ETMS/CIWS sectors had some aircraft with vertical rates. The largest vertical rate fraction observed within an individual sector was 0.85.

B. Modeling Vertical Motion Data

The model allows us to directly incorporate a particular mechanism by which vertical motion can increase workload. Workload grows when altitude uncertainty leads controllers to perceive a greater risk of air-to-air conflict. The model parameter that most directly reflects this uncertainty is the vertical separation threshold M_v used for calculating the mean conflict rate.

We previously used a global M_v of 1000 ft for all sectors. We now model the effect of vertical motion on capacity by defining an increasing linear relationship between the vertical motion fraction and the effective separation standard. When all aircraft in a sector fly level, the vertical separation threshold is 1000 ft. When aircraft in the sector change altitude, the effective vertical separation standard for the sector grows linearly. When all aircraft in the sector change altitude, the effective separation standard is M_{vmax}. Given the fraction F of aircraft in the sector with vertical motion of either type (F ranges from 0 to 1), the effective vertical separation threshold for the sector is

$$M_v = 1000 + F\,(M_{vmax} - 1000). \tag{6}$$

We determined M_{vmax} by searching for the value that gives the best agreement between model and measurement using the scoring rule described above. We found M_{vmax} to be about 2700 ft. Although the data allowed us to distinguish between ascending and descending aircraft, we did not make that distinction in the model.

The result of adding Eqn. 6 to the model is shown in Figures 4 and 5. As before, these figures plot the model capacities and the peak sector traffic counts, respectively as functions of sector volume, and then versus each other.

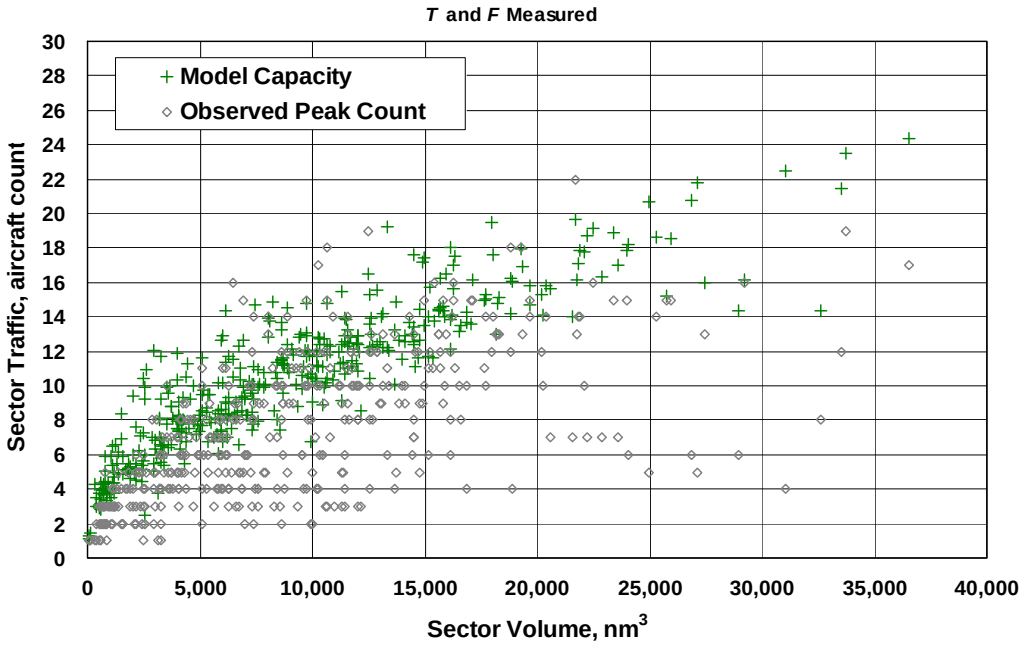

Figure 4. Peak counts and model capacities vs. sector volume when transit time *T* is measured directly and M_v is based on measurements of *F*.

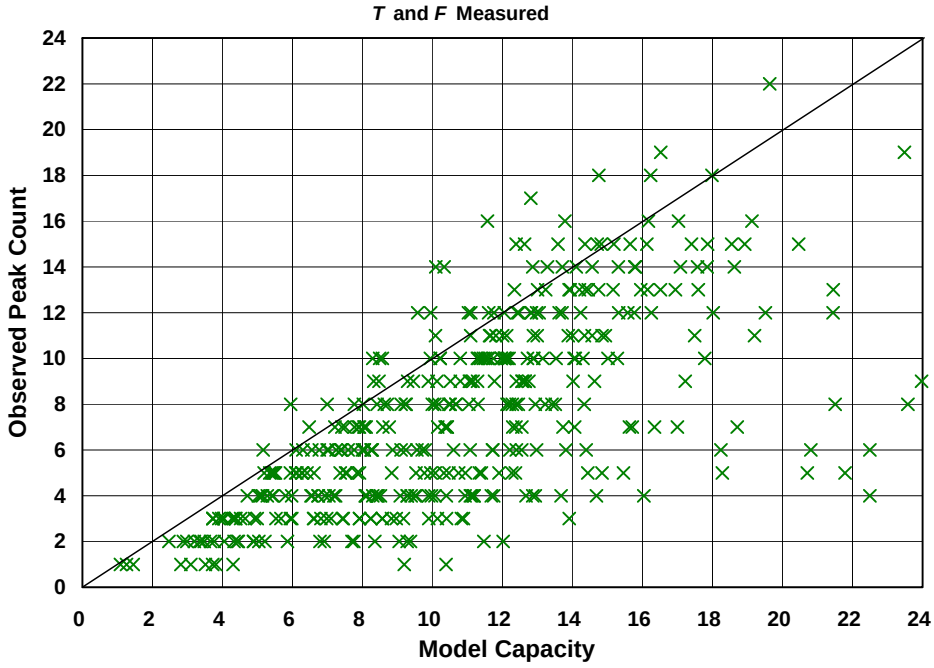

Figure 5. Count vs. model capacity when transit time *T* is measured directly and M_v is based on measurements of *F*.

The variable M_v correction increased the conflict rate and thereby reduced the capacity estimate relative to the original model for the 94% of the sectors that had climbing or descending aircraft. Consequently, it had the desired effect of decreasing the error for those whose peak traffic counts were lower than predicted by the original model. Conversely, it increased the error for a few sectors whose peak traffic counts were higher than predicted by the uncorrected model. The regression value for τ_c dropped from 82 s to 62 s to compensate for the growth in conflict rate.

Table 1 summarizes the quality-of-fit metrics for the three versions of the model. The model with measured T and variable M_v achieved the best overall fit. The addition of the simple linear growth factor appears to be a good predictor of sector capacity reduction relative to a model with a fixed vertical separation standard.

Table 1. Quality-of-Fit Metrics for Three Models.

Metric / Case	Perfect Fits $N_p = N_b$	Close Fits $\lvert N_p\text{-}N_b\rvert \leq 2$	High Counts $N_p > N_b+2$	Low Counts $N_p < N_b-2$	Score see Fig. 1
Estimate *T* from length	16	115	2	308	155
Measure *T*	22	169	4	252	229
Measure *T* and vary M_v	38	195	6	224	267

C. Heading and Speed Variance

We have also observed, in agreement with others,[9,12] that sectors with high peak counts tend to have more uniform flow. Organized flow results in lower closing speeds and hence lower conflict rates. In the limit, perfectly organized flow would eliminate all conflict workload, and sector capacity would be determined entirely by transit workload.

Given an appropriate measure of the organization of the flow, the model can account for this by reducing V_{12}. We have begun to evaluate candidate metrics based on the variance of the sector aircraft headings at the time of maximum demand. Preliminary results indicate that accounting for organized flow will reduce the number of sectors with high counts and further improve the model's quality-of-fit metrics.

D. Summary of Model Parameters for ETMS/CIWS Sectors

Table 2 summarizes the values of the global constants for the ETMS/CIWS sectors using the model with measured values of T and with M_v corrected to account for aircraft with vertical rates. These are preliminary results based on unofficial sector volumes. We intend to refine these results based on operational sector volumes for the entire NAS with measurements of traffic count, transit time, vertical rate fraction, heading distribution, and mean closing speed.

Table 2. Global Capacity Model Constants for ETMS/CIWS Sectors.

Constant	Value
G_b	0.1
τ_c	62 s
τ_r	0 s
τ_t	28 s
P	300 s
M_h	7 nautical miles (nm)
M_v	1000 ft
M_{vmax}	2700 ft
V_{12}	200 kt

IV. Monitor Alert Parameters

FAA Order 7210.3[15] defines the nominal MAP values as shown in Figure 6. The MAP rule explicitly defines maximum allowable operational sector loading based on "average sector flight time". It thus directly limits transit (i.e., inter-sector coordination) workload. According to the rule, "Average sector flight time will be calculated using data indicating functional position operations for a consecutive Monday through Friday, 7:00 AM – 7:00 PM local time frame."

The increasing region of the MAP curve is nearly linear and reflects queuing with workload intensity $G=\tau_t\,[N/T]$. The slope of the curve for flight times between 3 and 10 minutes is 1.714 aircraft/minute. If maximum sector loading occurs when G reaches 0.8, that slope implies a transit service time τ_t of 28 s. This is identical to the transit service time in Table 2.

The inconsistency between the airspace volumes of the ETMS/CIWS sectors and actual operational sectors prevents a meaningful comparison between model capacities and actual FAA MAP values for the ETMS/CIWS sectors. We have begun to compare operational MAP values with model capacities based on accurate operational

sector coordinates. We obtain the counts and the associated MAP values from the FAA Performance Data Analysis Reporting System (PDARS).[20]

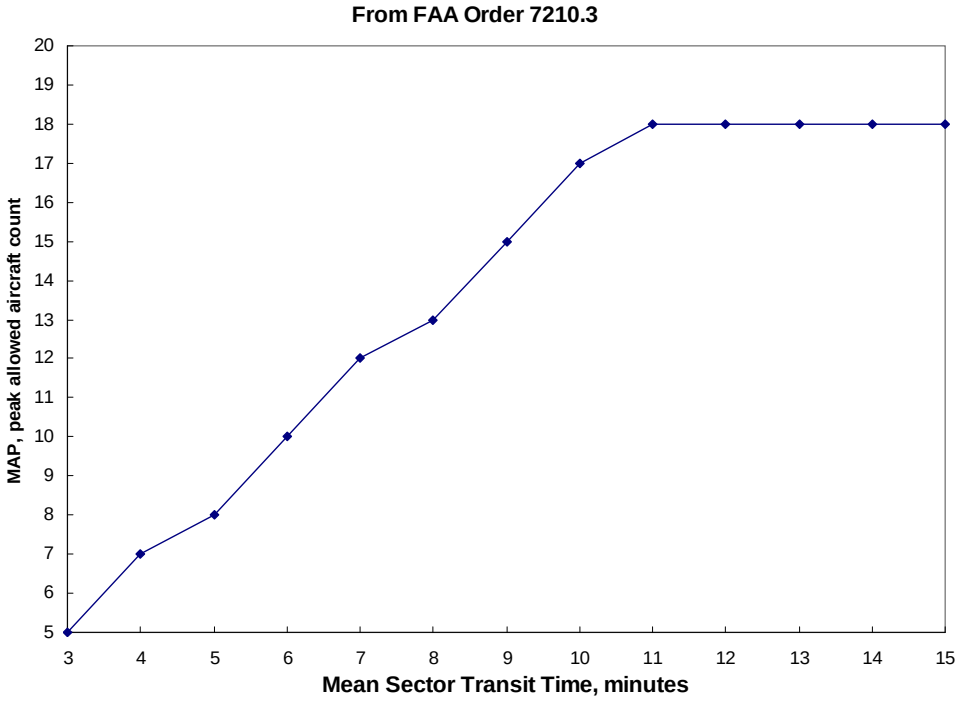

Figure 6. Monitor Alert Parameter density versus mean sector transit time.

Figure 7 plots initial results of this comparison showing the peak counts on 21 January 2007 for twenty-five en route sectors in ZNY as a function of sector volume. (We have omitted the four largest ZNY sectors for plotting clarity.) Superimposed on these counts are the official FAA MAP values in use that day for the same sectors. The Monitor Alert Parameters generally exceed the peak counts for smaller sectors and closely bound the peak counts for larger sectors. The agreement for large sectors reflects the effect of the eighteen-aircraft MAP limit on the operational traffic flow management process.

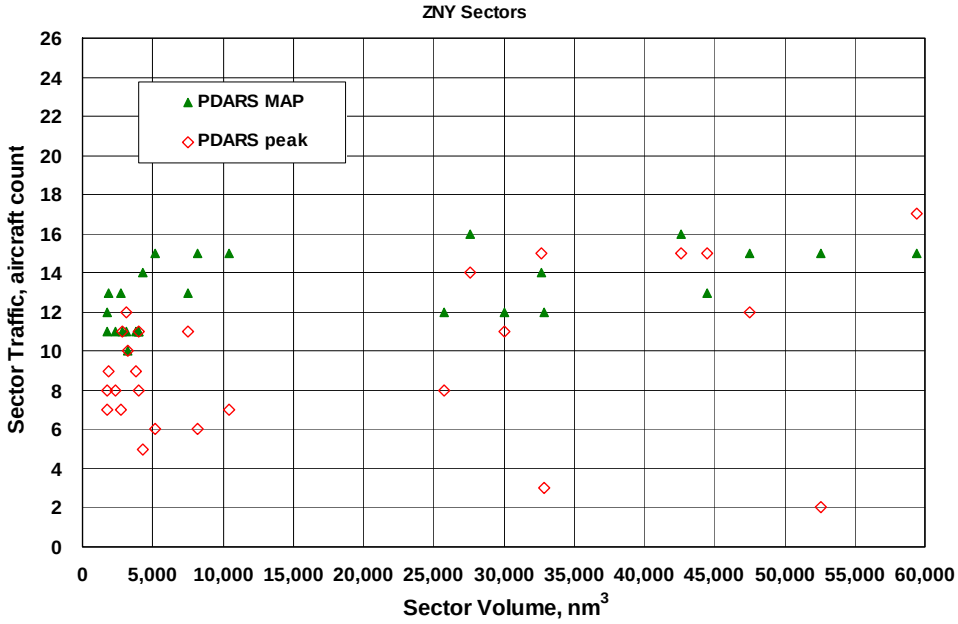

Figure 7. Peak traffic on 1/21/07 and MAP values for 25 ZNY sectors.

Figure 8 compares the ZNY peak count data with the predictions of our capacity model when applied to the ZNY sectors. We calculate model capacity using the parameters in Table 2. We use PDARS summary data to estimate the mean transit time *T* for each sector in the 20-minute period following the occurrence of the peak traffic count. We are not able to include a vertical separation standard correction because the PDARS summary data does not provide altitude change information.

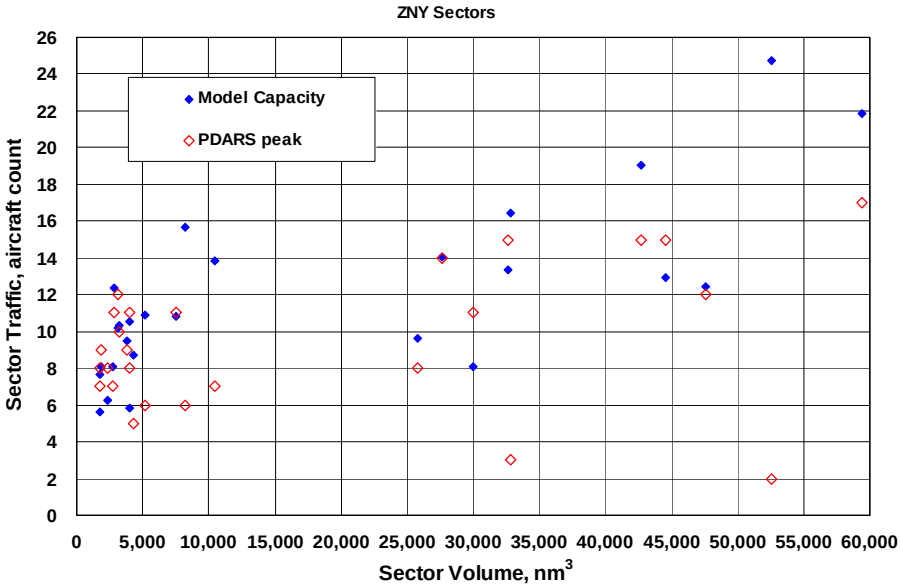

Figure 8. Peak traffic on 1/21/07 and model values for 25 ZNY sectors.

We used the scoring scheme of Figure 1 to first quantify the quality of the fit between the PDARS peak data and the model, and then between the PDARS peak data and the MAP rule. The overall model score and the MAP rule score are identical. The model results in more close-fit sectors, but the MAP rule results in more perfect fits.

For small sectors the model bounds the PDARS peak counts better than the MAP values because it accounts for growth in conflict workload with traffic density. The model generally exceeds the PDARS peak counts for larger sectors. The eighteen-aircraft MAP limit for sectors with long transit times tends to under-estimate the model predictions of actual safe capacity for large sectors.

V. Model Applications

The model provides a framework for understanding the capacity benefits of proposed new air traffic management technologies and operational procedures. The success of the model in predicting observed airspace loading bounds validates the interpretation of controller workload as a task-based queuing process. The model provides a structure for computing the capacity benefits of any proposed new technology or operational procedure. We take it as a fundamental postulate that future air traffic control procedures will continue to require human judgment for problem solving. Thus, research intended to increase capacity can focus either on reducing the rate of occurrence of controller tasks, or on reducing the time required to safely complete those tasks. Given a quantitative estimate of the rate or time reduction, the model can provide a numerical estimate of airspace capacity improvement.

One approach to reducing conflict rates is to improve communication, navigation, surveillance, and flight control technologies. Improving any one of these factors alone may provide some benefit. However, it has been shown[21] that a combination of improved communication for negotiating trajectories, improved navigation and flight control for adhering to trajectories, and improved surveillance for monitoring trajectory conformance could reduce both the rate of conflicts and the ease of resolution when they occur.

Considerable research is proceeding on decision support tools whose main goal is to reduce separation assurance service times.[22-26] Associated simulation studies have demonstrated significant capacity improvements. To maximize sector capacity, it is important to integrate such tools with technology and procedures that also reduce conflict occurrence rates.

Research also continues on communication technology and decision support tools to reduce inter-sector coordination service times.[27-29] Such technology might also facilitate intra-sector cooperation so that larger

controller teams could share responsibility within each sector. This would allow the use of larger sectors, which would further reduce inter-sector coordination loads.

The quadratic dependence of conflict rates on traffic density results in a synergistic relationship in which the total capacity increase from multiple technological or operational improvements can exceed the sum of the capacity increases from the individual improvements.

In Figure 9 we illustrate this synergy by computing the effect of hypothetical changes in conflict and transit workload on the capacity of the total ETMS/CIWS en route airspace. Here we define capacity as the sum of the model capacities for all of the ETMS/CIWS sectors. This definition is a simplification that does not account for regional throughput constraints from network flow. However, it serves as a useful illustrative construct.

The bottom curve shows the effect of a postulated reduction in conflict workload. Specifically, halving conflict workload would increase the total ETMS/CIWS capacity by 17%. The middle curve shows the effect of a postulated reduction in transit workload. Reducing transit workload by 50% would cause the total ETMS/CIWS capacity to grow by 32%. That, plus a halving of the conflict workload, would increase the total ETMS/CIWS capacity by 67%, as shown in the upper curve. The quadratic workload relationship makes this exceed the sum of the two individual capacity increases, which is only 49%. This illustrates the importance of addressing both conflict and transit workload.

An ability to forecast capacity changes under changing operational conditions could help reduce aircraft operating costs and improve the efficiency of the controller workforce. Airspace planners often estimate capacity using microscopic workload simulations. However, the cost and complexity of those models limit their use in tactical airspace planning. The analytical nature of the model allows rapid computation for real-time operational airspace redesign. It has been noted[30] that dynamic capacity estimates could help re-route aircraft when storms or other disturbances change effective sector volumes, when controllers vector traffic, or when vertical motion increases conflict workload. The model can account for these effects by modifying transit times, airspace volumes, closing velocities, and separation standards. The model results show quantitatively that today's aircraft count in more than half of the ETMS/CIWS sectors peaks at capacity during high-demand summer periods. This explains the disruptive delays that occur when summer storms reduce sector capacities during busy periods.

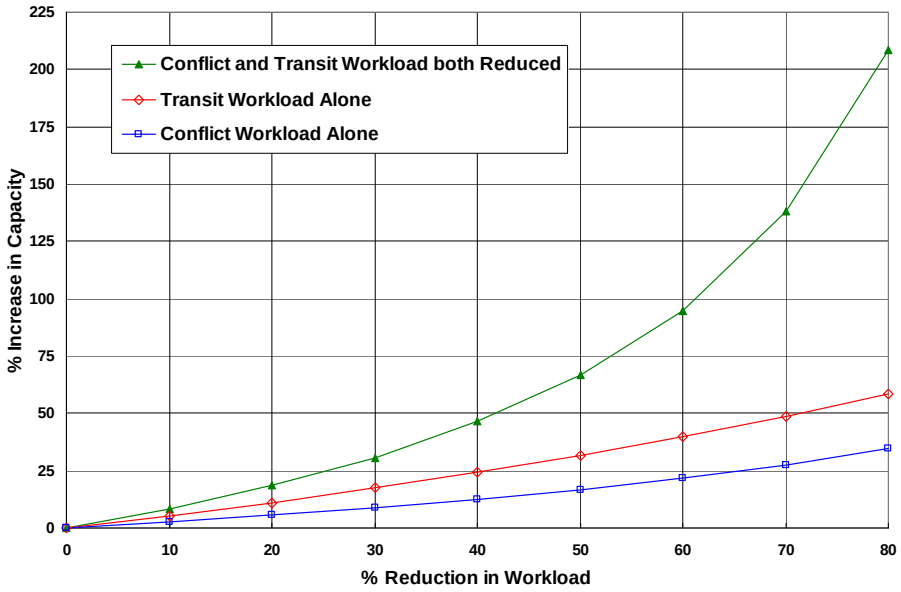

Figure 9. Effect of workload reduction on total capacity increase for all ETMS/CIWS sectors.

The model also allows us to examine individual workload components for en route sectors. Figure 10 is a plot of the transition and conflict workload components for the ETMS/CIWS sectors when operating at capacity. The scatter is caused by local variations in sector transit time T and vertical separation standard M_v.

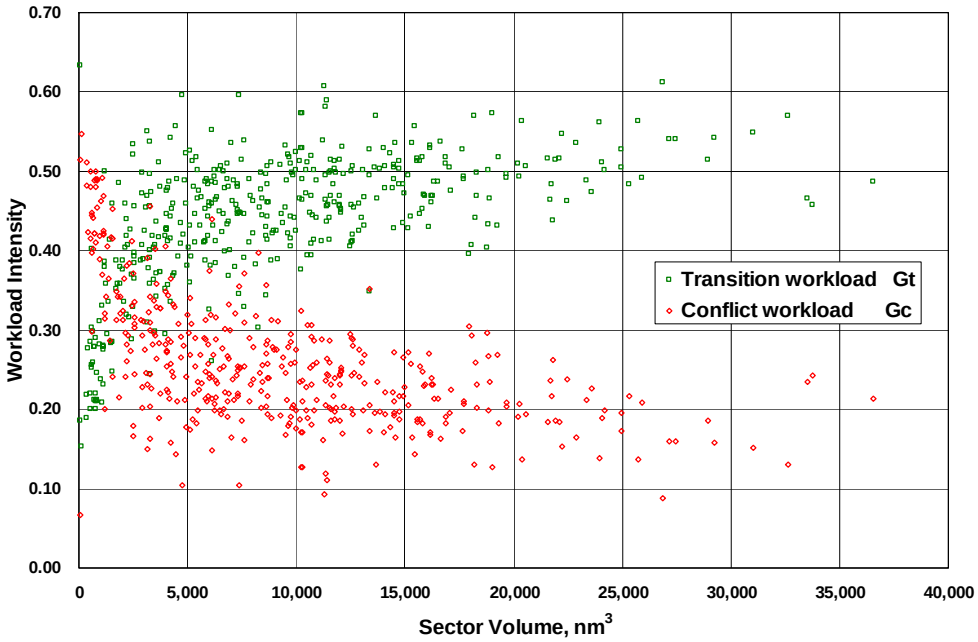

Figure 10 ETMS/CIWS Sector workload components at capacity.

These data series have complementary trends because, at capacity, the workload equation is a fixed-sum calculation. Transit workload dominates in sectors larger than about 2,000 cubic nautical miles. As sector volume increases, the conflict workload component decreases, and the transition workload component increases. High traffic densities cause conflict workload to dominate in very small sectors. This is contrary to conventional wisdom, which identifies inter-sector coordination workload as the main barrier to reducing sector size.

VI. Conclusion

The Monitor Alert Parameters used to define the peak allowable traffic in en route sectors in the United States account only for workload from inter-sector coordination tasks. We have shown that a more complete model that also accounts for workload from conflict avoidance provides a numerical bound for capacity in close agreement with peak observed sector traffic. The analytical nature of the model allows us to infer mean controller service times for coordination and separation tasks by fitting against peak traffic counts from large numbers of en route sectors.

One can improve the model fit by replacing global model parameters with sector-specific parameters based on traffic measurements from individual sectors. We first obtained an exact value for mean transit time by direct observation of tracks in peak traffic periods. We then accounted for increases in conflict workload caused by altitude uncertainty by measuring the daily fraction of aircraft tracks with vertical motion. Both of these metrics improved the agreement between observed traffic peaks and the model bound. We anticipate that a measure of traffic flow uniformity will further improve the model fit.

The agreement between model and measurement proves the hypothesis that workload limits capacity. The model provides quantitative insight into the tradeoff between operational capacity benefits and efficiency costs of changing sector sizes. We have illustrated the use of the model to predict the capacity benefits of hypothetical air traffic management technology and operational improvements. The results indicate that technology and automation aids should focus on reducing both transit and conflict workload.

Acknowledgement

This work is sponsored by NASA Ames under Air Force Contract #FA8721-05-C-0002. Opinions, interpretations, recommendations, and conclusions are those of the authors and are not necessarily endorsed by the United States Government.

References

1. Sridhar, Sheth, and Grabbe, "Airspace Complexity and its Application in Air Traffic Management," *2nd USA/Eurocontrol ATM Seminar*, Orlando Florida, 1998.
2. Laudeman, Sheldon, Branstrom, and Brasil, "Dynamic Density: An Air Traffic Management Metric," NASA-TM-1998-112226, 1998.
3. Delahaye and Puechmorel, "Air Traffic Complexity: Towards Intrinsic Metrics," *3rd USA/Europe ATM Seminar*, Napoli, Italy, 2000.
4. Histon, Aigoin, Delahaye, Hansman, and Puechmorel, "Introducing Structural Considerations into Complexity Metrics," *4th USA/Europe ATM Seminar*, Santa Fe, NM, 2001.
5. Chatterji and Sridhar, "Measures for Air Traffic Controller Workload Prediction," *1st AIAA Aircraft Technology, Integration, and Operations Forum*, Los Angeles, CA, 2001.
6. Majumdar, Ochieng, and Polak, "Estimation of Capacity of European Airspace from a Model of Controller Workload," *J. Navigation*, 55, 381-403, 2002.
7. Kopardekar and Magyarits, "Measurement and Prediction of Dynamic Density," *5th USA/Europe Air Traffic Management R&D Seminar*, Budapest, June 2003.
8. Masalonis, Callaham, and Wanke, "Dynamic Density and Complexity Metrics for Real Time Traffic Flow Management," *5th USA/Europe Air Traffic Management R&D Seminar*, Budapest, 2003.
9. Hilburn, B., "Cognitive Complexity in Air Traffic Control - A Literature Review," EEC Note No. 04/04: Eurocontrol, 2004.
10. Majumdar, Ochieng, McAuley, Lenzi, and Lepadatu, "The Factors Affecting Airspace Capacity in Europe: A Framework Methodology Based on Cross Sectional Time-Series Analysis Using Simulated Controller Workload Data," *6th USA/Eurocontrol ATM R&D Seminar*, Baltimore, June 2005.
11. Kopardekar, Schwartz, Magyarits, and Rhodes, "Airspace Complexity Measurement: An Air Traffic Control Simulation Analysis", *7th USA/Europe Air Traffic Management R&D Seminar*, Barcelona, 2-5 July 2007.
12. Song, Wanke, and Greenbaum, "Predicting Sector Capacity for TFM," *7th USA/Europe Air Traffic Management R&D Seminar*, Barcelona, 2-5 July 2007.
13. Lee, Feron, and Pritchett, "Air Traffic Complexity: An Input-Output Approach," *7th USA/Europe Air Traffic Management R&D Seminar*, Barcelona, 2-5 July 2007.
14. Zelinski and Romer, "Estimating Capacity Requirements for Air Transportation System Design," *7th USA/Europe Air Traffic Management R&D Seminar*, Barcelona, 2-5 July 2007.
15. FAA Order 7210.3, Facility Operation and Administration, Sec. 7, 30 Aug 2007. http://www2.faa.gov/airports_airtraffic/air_traffic/publications/atpubs/FAC/Ch17/s1707.html
16. Welch, Andrews, Martin, and Sridhar, "Macroscopic Workload Model for Estimating En Route Sector Capacity," *7th USA/Europe Air Traffic Management R&D Seminar*, Barcelona, 2007.
17. Schmidt, "A Queuing Analysis of the Air Traffic Controller's Work Load," *IEEE Trans. Systems, Man, Cybernetics*, Vol. SMC-8, No. 6, 1978.
18. Andrews and Welch, "Workload Implications of Free Flight Concepts," *1st USA/Eurocontrol ATM Seminar*, Saclay, France, 1997.
19. Evans, and Ducot, "Corridor Integrated Weather System," *Lincoln Laboratory Journal*, Vol. 16, No. 1, 2006 pp. 59-80.
20. den Braven and Slade, "Concept and Operation of the Performance Data Analysis and Reporting System," Paper 2003-01-2976, *SAE Advances in Aviation Safety Conference (ACE)*, Montreal, September 2003.
21. Andrews, Welch, and Erzberger, "Safety Analysis for Advanced Separation Concepts," *6th USA/Eurocontrol ATM R&D Seminar*, Baltimore, June 2005.
22. Kirk, Heagy, and Yablonski, "Problem Resolution Support for Free Flight Operations," *IEEE Transactions on Intelligent Transportation Systems*, Volume 2, No. 2, June 2001.
23. McNally and Gong, "Concept and Laboratory Analysis of Trajectory-Based Automation for Separation Assurance," *AIAA GNC Conference*, Colorado, 2006.
24. Farley and Erzberger, "Fast-Time Simulation Evaluation of a Conflict Resolution Algorithm Under High Air Traffic Demand," *7th USA/Europe Air Traffic Management R&D Seminar*, Barcelona, 2007.
25. Celio and Smith, "Performance Based Air Traffic Management," *7th USA/Europe Air Traffic Management R&D Seminar*, Barcelona, 2007.
26. Farley, Kupfer, and Erzberger, "Automated Conflict Resolution: A Simulation Evaluation Under High Demand Including Merging Arrivals," *7th AIAA ATIO Conference*, Belfast, 2007.

[27] Kerns, and McFarland, "Conflict Probe Operational Evaluation and Benefits Assessment," MP98W239, MITRE Corporation, November 1999.
[28] Leiden and Green, "Trajectory Orientation: A Technology-Enabled Concept Requiring a Shift in Controller Roles and Responsibilities," *3rd USA/Europe ATM Seminar*, Napoli, Italy, 2000.
[29] Bolic and Hansen, "User Request Evaluation Tool (URET) Adoption and Adaptation, Three Center Case Study," *6th USA/Europe ATM Seminar*, Baltimore, MD, June 2005.
[30] Klein, Kopardekar, Rodgers, and Kaing, "'Airspace Playbook': Dynamic Airspace Reallocation Coordinated with the National Severe Weather Playbook," *7th AIAA ATIO Conference*, Belfast, 2007.